Eur. Phys. J. C (2013) 73:2649
DOI 10.1140/epjc/s10052-013-2649-6

THE EUROPEAN PHYSICAL JOURNAL C

Special Article - Tools for Experiment and Theory

Fabrication, testing and simulation of a high spatial resolution alpha-particle imager based on ZnO nanowires in a polycarbonate nanoporous membrane

Ali Taheri[a], **Shahyar Saramad**[b], **Samira Ghalenoi**[c], **Saeed Setayeshi**[d]

Faculty of Energy Engineering and Physics, Amirkabir University of Technology, Tehran, Iran

Received: 19 May 2013 / Revised: 4 October 2013 / Published online: 28 November 2013

Abstract A new architecture consisting of ZnO nanowires embedded in a polycarbonate nanoporous membrane was proposed, fabricated and simulated as a high spatial resolution alpha particle imager. The experimental and Geant4 simulation results showed that ZnO nanowires could act as scintillating fibers to prevent spread of the generated optical photons inside the imager. This property can be used to precisely determine alpha collision coordinates. An array of these nanowires can be also applied as a new high spatial resolution alpha particle imager.

1 Introduction

Monitoring flux of alpha particles using techniques such as autoradiography and imaging plates plays an important role in detecting radioactive nuclides and polluted parts in the processing facilities which generate uranium and plutonium [1, 2]. It is very essential to design a monitoring system which is capable of extracting precise information on energy, direction, flux, etc. of alpha particles. Recently, many researchers have attempted to introduce a compact and portable alpha imager based on scintillator crystals combined with a position sensitive detector to provide real time monitoring of alpha and probably other heavy charged particles [3]. In designing such a monitoring system, ZnO has attracted attention as a scintillating material. ZnO has promising properties [3–9] including high internal quantum efficiency, short decay time, good linearity, fast decay time below 1 ns [10, 11], high radiation hardness, lack of toxicity, medium ionization energy of 9.0 eV and small fano-factor [12–14]. More recently, ZnO in the form of nanowires has been proposed as a high spatial resolution X-ray detector [15, 16].

In this work, a new scintillating screen based on ZnO nanowires was introduced as a high spatial resolution imager to monitor alpha particles. The proposed electrochemically synthesized imager consisted of ZnO nanowires embedded in a polycarbonate nanoporous membrane. In this structure, each nanowire could act as a scintillating fiber guiding the generated optical photons to end of the detector along the particle path inside the detector.

Using Monte Carlo simulations, ability of the proposed structure as a high spatial resolution imager was evaluated. The simulations were performed by Geant4 toolkit [17], which was capable of considering the interaction of high energy particles with matter and transport of the optical photons generated inside the scintillating crystals. Scintillation and optical response of the fabricated screen were tested by a photomultiplier tube (PMT) and its spatial resolution was extracted by a charge coupled device (CCD) sensor.

2 Material and methods

2.1 Detection setup and principles

The detector's assembly is illustrated in Fig. 1. It consisted of a 10 μm thick polycarbonate membrane with pore diameter of 200 nm. The membrane's pores were filled with ZnO to form nanowires. Due to the manufacturing process of a real polycarbonate membrane, its pores are not ideally perpendicular to the membrane surface, which was considered in the simulation [18]. The membrane's pores had maximum tilt angle of 30° with respect to normal vector of the membrane's surface. Porosity of the membrane was 6×10^8 pores/cm^2. This structure was called "the Nanowire Based Detector" (NWD).

[a] e-mail: at1361@aut.ac.ir, at1361@gmail.com
[b] e-mail: ssaramad@aut.ac.ir
[c] e-mail: s.ghalenoi@aut.ac.ir
[d] e-mail: setayesh@aut.ac.ir

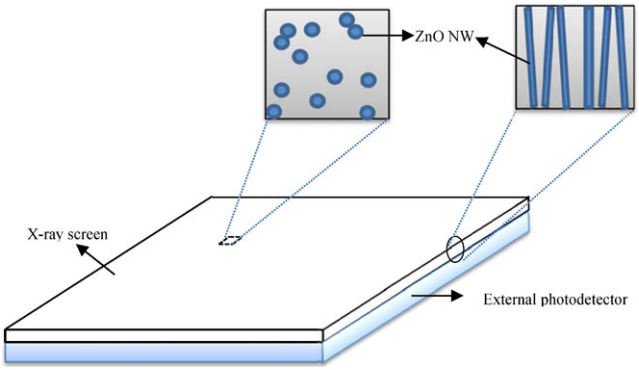

Fig. 1 Structure of the NWD

The light spreading inside the NWD was expected to decrease due to the light guiding effect of the nanowires. The nanowires acted as optical fibers in the NWD. Since the membrane had a different refractive index from ZnO, the optical photons which had incident angle of smaller than critical angle were reflected and guided to the end of the nanowires and others were scattered inside the detector. Also, some of the generated optical photons might be absorbed inside the detector.

2.2 Monte Carlo simulation

2.2.1 Geant4 setting

To perform the simulation, previous simulation methods were strictly followed [15, 16]. Geant4 (version 4.9.4) was employed to perform the Monte Carlo simulation. Geant4 simulation toolkit includes a series of packages to simulate electromagnetic interactions of particles with matter and is specialized for different particle types, energy range and specific physics models. To simulate the whole process of detection for alpha particles, the physics list includes low energy electromagnetic physics, scintillation and transportation of optical photons. The G4EMLOW 6.23 data library, which is low-energy electromagnetic (EM) package containing data files for EM processes down to very low energies (eV scale), was used in this simulation. The UNIFIED model in Geant4 was also applied for modeling reflection of photons at surfaces between two dielectric materials [19–21]. In photon reflection modeling, surface roughness between the dielectrics was neglected.

2.2.2 Input optical parameters

Accurate Geant4 simulation of ZnO scintillator required optical properties of ZnO such as absolute light yield, emission spectrum, optical absorption length, optical scattering length and refractive index to be included to the modeling. Refractive indexes of ZnO for different wavelengths ranging from 300 to 900 nm were extracted from [22]. Scintillation light yield of ZnO was set to 9000 photon/MeV [23]. Also, X-ray induced luminescence spectrum and optical absorption/scattering coefficients of ZnO were similar to what previously reported in [24, 25]. The parameters required for modeling light transport in the polycarbonate included its refractive index, optical scattering length and absorption length [26–28].

2.3 Experimental setup

2.3.1 Synthesis of aligned ZnO nanowires

Typical synthesis of the nanowires was carried out by electrodeposition of ZnO in a polycarbonate membrane. Average pore diameter, pore density and thickness of the polycarbonate membrane (Whatman) used in this experiment were 200 nm, 6×10^8 pores/cm^2 and $\sim$10 μm, respectively. In order to ensure a good electrical contact for electrodeposition, a 60 nm gold layer was sputtered on the membrane's bottom in rate of $\sim$26 nm/min. Electrodeposition system was based on a classical three-electrode apparatus. A saturated silver/silver chloride electrode (Ag/AgCl in saturated KCl) was used as the reference and connected via a salt bridge. A stainless steel plate (high purity) served as the anode. The electrolyte used for fabrication of ZnO nanowires was 0.05 M, $Zn(NO_3)_2{\cdot}6H_2O$ (99 %, Chem-Lab). Copper tape served as the cathode substrate for the nanowires' growth. Electrodeposition was carried out at 1 V and 70 °C for 3800 s.

2.3.2 Characterization

The synthesized ZnO nanowires were examined by X-ray diffraction (XRD) and scanning electron microscopy (SEM) analyses for structural and morphological identification. Thin film XRD spectrum of ZnO nanowires was obtained perpendicular to the growth direction on a Thermo Electron diffractometer (Inel-EQUINOX3000) operating in the θ–2θ Bragg configuration by using a Cu-Kα X-ray source with a step size of 0.031° and a wavelength of 1.541874 Å. Figure 2 presents the XRD data for the sample. It describes the crystalline nature of the ZnO nanowires with the peaks correspond to reflection from 100, 002, 101, 102 and 103 crystal planes. All the peaks could be indexed to ZnO hexagonal phase with a Wurtzite structure and unit cell parameters of equal to $a = b = 3.285$ Å and $c = 5.126$ Å. According to the XRD result, the nanowires had a polycrystalline nature with particle size of around 20 nm, which could be estimated from full width at half maximum (FWHM) of the XRD peaks using Scherer formula [29].

A top image of the nanowire arrays grown in the template (Fig. 3a) was observed by SEM (Seron-AIS2100). To obtain

this SEM image, the membrane was dried in air followed by brief etching in chloroform (SeccoSolv®, Merck). In addition, to extract length of the nanowires, the membrane was completely dissolved in chloroform. The resulted SEM image is shown in Fig. 3b. As demonstrated in this figure, the nanowires had average length of about 10 μm.

2.3.3 Testing setup and methods

PMT test A Hamamatsu PMT (R1828-01) was used to survey scintillation behavior of the fabricated screen in the presence of alpha particles. For this purpose, the sample was attached to the PMT and its optical response was recorded for 300 s by a multichannel analyzer (MCA) with and without an alpha particle source. The difference between the recorded results showed scintillation response of ZnO nanowires to alpha particles.

CCD test To extract spatial resolution of the fabricated screen, it was attached to a 5 mega pixel CCD (sensitive to ultraviolet photons) with pixel size of about 2 μm. A collimated alpha emitter (^{238}Pu) was placed in front of the nanowire-based screen. The setup was optically sealed and an image was taken by the CCD sensor. To evaluate the background noise, an image without alpha particle source was also taken. Based on this information, alpha particle interaction point with the detector and also strength of scintillation and spatial resolution of the fabricated imager were extracted.

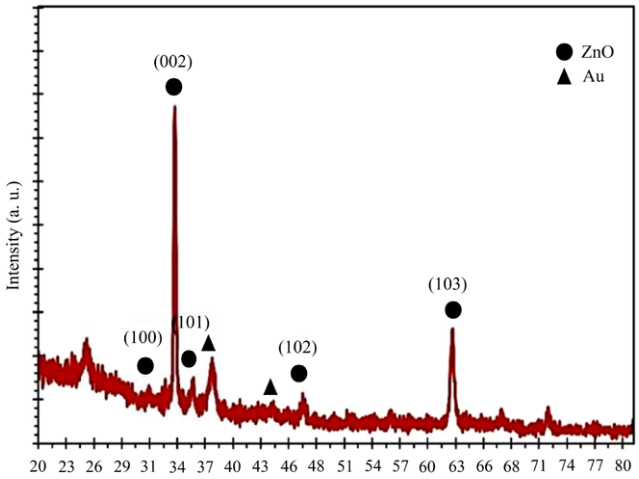

Fig. 2 XRD diffractogram measurement made perpendicular to growth direction of electrochemically grown ZnO nanowires at 70 °C and 1 V for 3800 s

3 Results and discussion

3.1 Simulation results

Surface dimensions and thickness of the simulated NWD were considered 2×2 cm^2 and 5–20 μm, respectively. Simulation was done using a 5.5 MeV pencil beam alpha particle source. Alpha particles impinged at the detector center, parallel to the normal vector of the detector surface. Projection of the output light from backside of the detector was recorded to extract spatial resolution. Figure 4 shows the simulated projections for the NWD with thickness of 5, 10, 15 and 20 μm.

The projections showed an increase in spreading the output light with increasing the detector thickness, which was because increase in the detector thickness increased spreading probability of the optical photons inside the nanowires. To investigate performance of the proposed imager (Fig. 1), the simulation results were compared with a single crystal ZnO detector, called "Macro Detector" (MD), which was the same size as the NWD. The generated optical photons inside the MD could spread to any direction inside the detector and this problem could affect spatial resolution of the detector. The same simulation was also performed for the MD and the results are shown in Fig. 5.

As shown in this figure, for different thicknesses, the light spreading in output of the MD dramatically increased in comparison with the NWD (Fig. 4). To understand role of the nanowires in preventing spread of the optical photons,

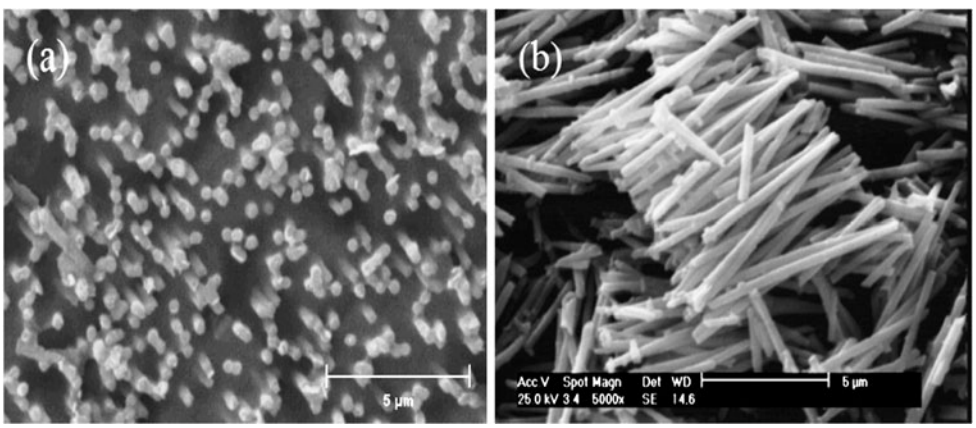

Fig. 3 SEM image of ZnO nanowires grown at 70 °C and 1 V for 3800 s: (**a**) top view of the nanowires after brief etching of the membrane, (**b**) observed length of the nanowires after complete removal of the membrane

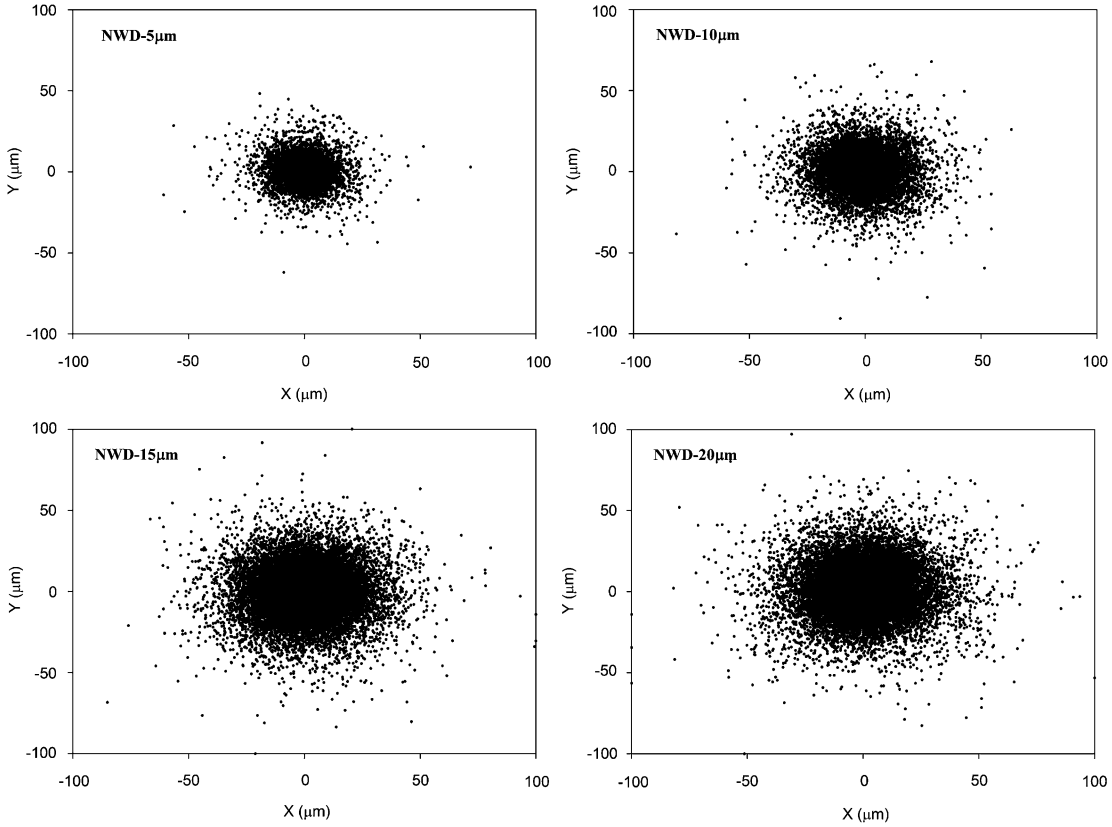

Fig. 4 Simulated projections for different thicknesses (5, 10, 15 and 20 μm) of the NWD in a 200 × 200 μm^2 scale

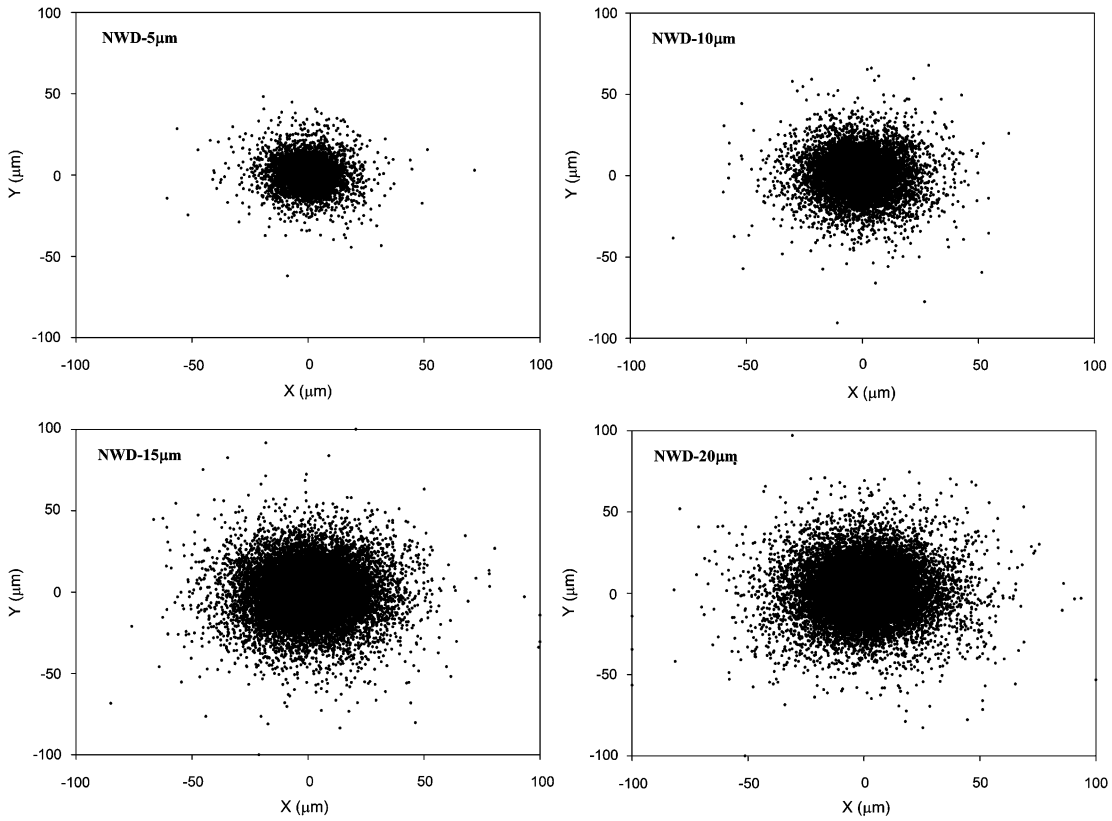

Fig. 5 Simulated projections of a 2 × 2 cm^2 MD for different thicknesses of 5, 10, 15 and 20 μm

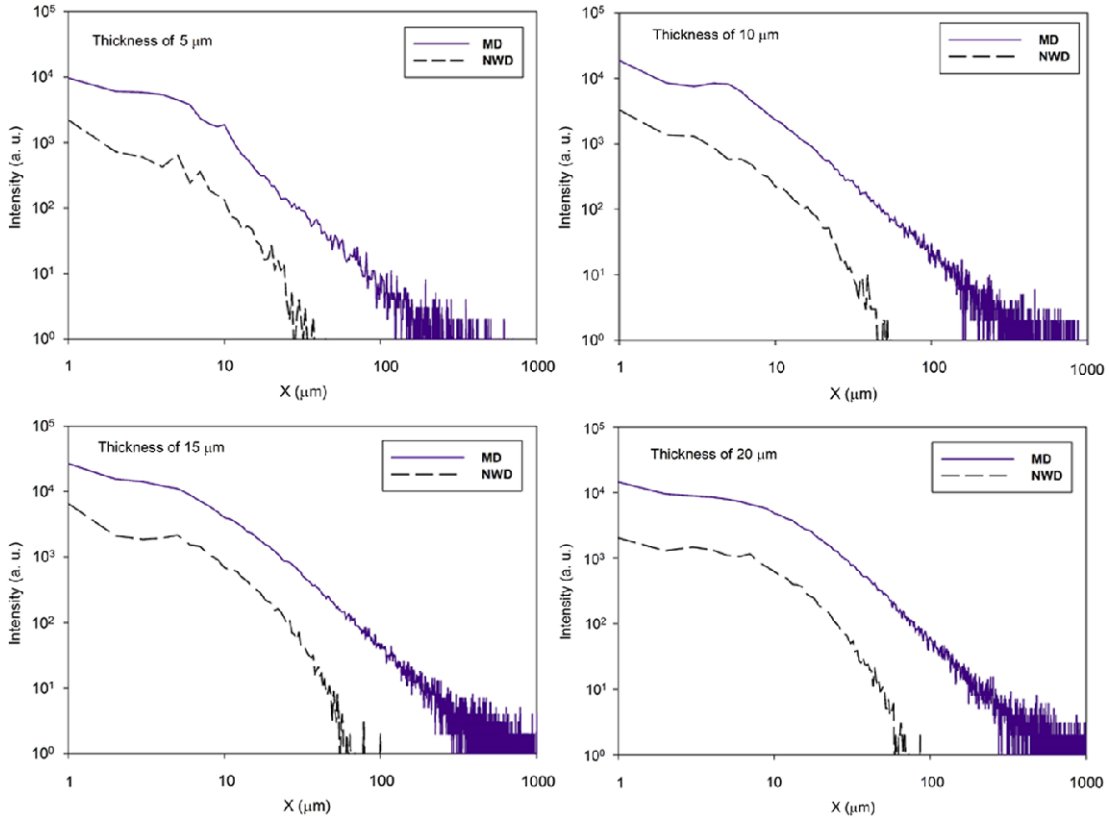

Fig. 6 Radial distribution of the light intensity extracted from the projections at different detector thicknesses (*solid lines* indicate the MD and dashed lines indicate the NWD)

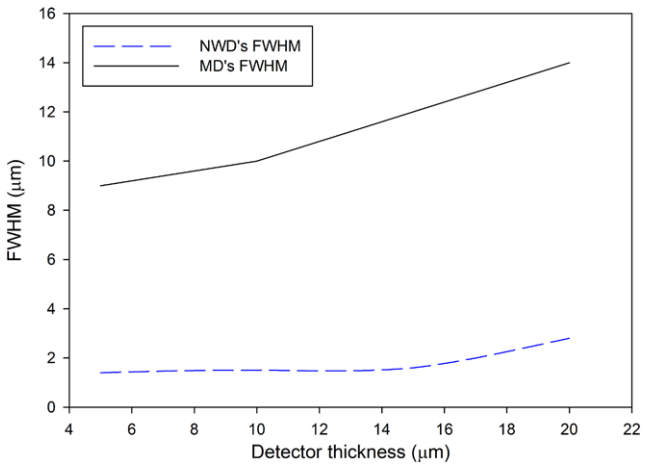

Fig. 7 FWHM (μm) of spatial resolution of the NWD and MD as a function of the detector thickness

radial distribution of light intensity was also extracted as a function of thickness, the results of which are shown in Fig. 6. According to this figure, the light spreading at the backside of the NWD was less than 100 μm; but, it was around 1 cm for the MD.

Figure 7 shows FWHMs of spatial resolutions for the simulated geometries, which were carried out with different detector thicknesses. The results presented in Fig. 7 show enhancement of FWHM of the NWD compared to the MD. FWHM of the spatial resolution for the NWD with thickness of 10 μm was about 5 times smaller than that of the MD.

Table 1 The number of recorded counts using the PMT during 300 s related to scintillation of the ZnO nanowires and background

Background and scintillation	Background	Scintillation
145128	13578	131550

3.2 Experimental results

3.2.1 Results of PMT test

To test performance of the imager, the number of net alpha detections from a 2.775 kBq ^{238}Pu source during 300 s was measured by a combination of the NWD and an ultraviolet sensitive PMT. The recorded counts in 1024 channels of the MCA during 300 s related to scintillation of ZnO nanowires and background are represented in Table 1.

Figure 8 shows a recorded spectrum in the first 150 channels of the MCA for the background and scintillation counts during 300 s.

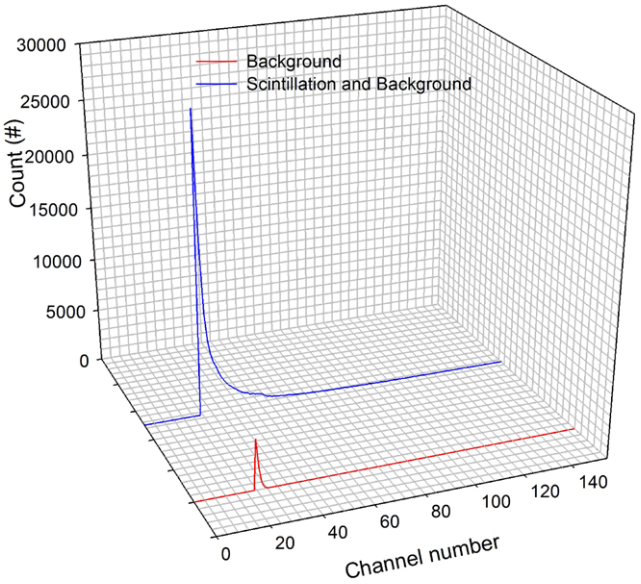

Fig. 8 Recorded spectrum in the first 150 channels of the MCA for background and scintillation counts during 300 s

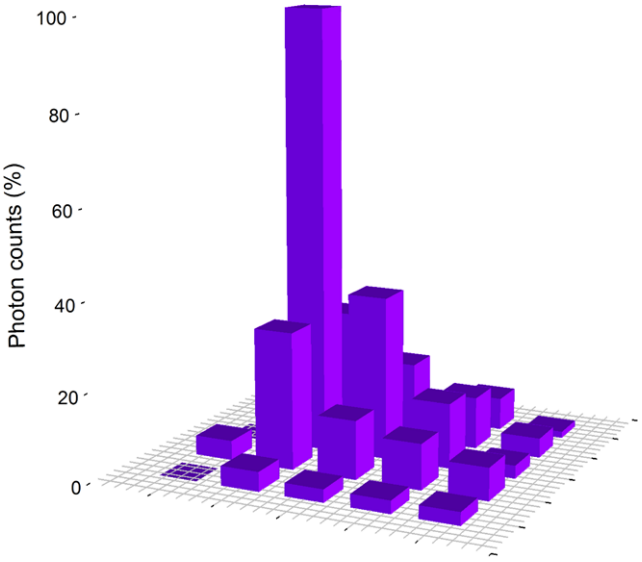

Fig. 9 The number of optical photons recorded in each pixel of CCD for a short shot during incident of alpha particles

The results showed that, out of 832500 emitted alpha particles, around 131500 ones were detected, which meant that quantum efficiency of the detector was around 16 %. This efficiency was close to ratio of total nanowires cross-section area to the sample surface area.

3.2.2 Results of CCD test

For assessing spatial resolution of the imager, the number of optical photons was recorded in each pixel of a five mega pixel CCD. The obtained results showed that FWHM of spatial resolution of the NWD was less than a single pixel dimension (1.86 μm). The number of optical photons recorded in each pixel of the CCD considering effect of background for a typical imaging is shown in Fig. 9. In this figure, a pixel located in row 467 and column 2480 had maximum intensity and its neighboring pixels had intensities of lower than half of the maximum; i.e. for thickness of 10 μm, FWHM of spatial resolution of the fabricated imager was less than 2 μm, which was in good agreement with the simulation results (Fig. 7).

4 Conclusion

The results showed that ZnO nanowires in a polycarbonate membrane could act as a high spatial resolution alpha particle detector. The experimental data demonstrated good agreement with simulation results, indicating that the proposed imager had less than 2 μm FWHM of spatial resolution, which was about 5 times smaller than the bulk scintillator. Nonetheless, for the same thickness of ZnO, the NWD had smaller detection efficiency compared to the MD, because the NWD had less scintillation material. A higher density of the nanowires could overcome this drawback.

References

1. K. Sakasai, M. Katagiri, M. Kishimoto, T. Nakamura, K. Toh, H. Takahashi, M. Nakazawa, Readout characteristics of an imaging plate by fast laser pulses. IEEE Trans. Nucl. Sci. **47**, 944 (2000)
2. J. Simonović, J. Vuković, R. Antanasijević, Nucl. Instrum. Methods Phys. Res., Sect. A **147**, 141 (1977)
3. T. Yanagida et al., Evaluations of ZnO based α-ray imager. IEEE Nucl. Sci. Symp. Conf. Record (NSS/MIC) 188 (2010)
4. J.S. Neal et al., Evaluation of melt-grown, ZnO single crystals for use as alpha-particle detectors. IEEE Trans. Nucl. Sci. **55**(3), 1397 (2008)
5. J.S. Neal et al., Investigation of ZnO-based polycrystalline ceramic scintillators for use as α-particle detectors. IEEE Trans. Nucl. Sci. **56**(3), 892 (2009)
6. T. Yanagida et al., Scintillation properties of in doped ZnO with different in concentrations. IEEE Trans. Nucl. Sci. **57**(3), 1325 (2010)
7. C. Liang et al., Experimental study on scintillation efficiency of ZnO: in to proton response. Chin. Phys. C **35**(11), 1037 (2011)
8. M. Lorenz et al., Fast, high-efficiency, and homogeneous room-temperature cathodoluminescence of ZnO scintillator thin films on sapphire. Appl. Phys. Lett. **89**, 243510 (2006)
9. J.S. Neal et al., Comparative investigation of the performance of ZnO-based scintillators for use as a-particle detectors. Nucl. Instrum. Methods Phys. Res., Sect. A **568**(2), 803 (2006)
10. U. Ozgur et al., A comprehensive review of ZnO materials and devices. J. Appl. Phys. **98**, 041301 (2005)

11. T. Nakazato et al., Hydrothermal-method-grown ZnO single crystal as fast EUV scintillator for future lithography. J. Cryst. Growth **311**, 875 (2009)
12. J. Wilkinson, K.B. Ucer, R.T. Williams, Picosecond excitonic luminescence in ZnO and other wide-gap semiconductors. Radiat. Meas. **38**, 501 (2004)
13. F.D. Auret, S.A. Goodman, M. Hayes, M.J. Legodi, H.A. van-Laarhoven, D.C. Look, Electrical characterization of 1.8 MeV proton-bombarded ZnO. Appl. Phys. Lett. **79**(19), 3074 (2001)
14. R.C. Alig, S. Bloom, C.W. Struck, Scattering by ionization and phonon emission in semiconductors. Phys. Rev. B **22**(12), 5565 (1980)
15. A. Taheri, S. Saramad, S. Setayeshi, Geant4 simulation of zinc oxide nanowires in anodized aluminum oxide template as a low energy X-ray scintillator detector. Nucl. Instrum. Methods Phys. Res., Sect. A **701**, 30 (2013)
16. A. Taheri, S. Saramad, S. Setayeshi, ZnO nanowires in polycarbonate membrane as a high resolution X-ray detector (A Geant4 simulation). Nucl. Instrum. Methods Phys. Res., Sect. A **716**, 15 (2013)
17. S. Agostinelli et al., Geant4-a simulation toolkit. Nucl. Instrum. Methods Phys. Res., Sect. A **506**, 250 (2003)
18. V.P. Menon, C.R. Martin, Fabrication and evaluation of nanoelectrode ensembles. Anal. Chem. **67**, 1920 (1995)
19. A. Levin, C. Moisan, A more physical approach to model the surface treatment of scintillation counters and its implementation into DETECT. IEEE Nucl. Sci. Symp. Conf. Record **2**, 702 (1996)
20. Geant4 Collaboration, Physics reference manual. Available online at http://wwwasd.web.cern.ch/wwwasd/geant4/geant4.htmlS
21. S.K. Nayar, K. Ikeuchi, T. Kanade, Surface reflection: physical and geometrical perspectives. IEEE Trans. Pattern Anal. Mach. Intell. **13**, 611 (1991)
22. M. Bass, *Handbook of Optics, Vol. 2: Devices, Measurements, and Properties*, 2nd edn. (McGraw-Hill, New York, 1994)
23. E.I. Gorokhova et al., Optical, luminescence, and scintillation properties of ZnO and ZnO: Ga ceramics. J. Opt. Technol. **75**, 741 (2008)
24. X. Yang, Electrical and optical properties of zinc oxide for scintillator applications. Ph.D. thesis, University of Virginia (2008). https://eidr.wvu.edu/eidr/documentdata.eIDR?documentid=5909
25. L. Xin-Hua et al., Electrical and optical properties of bulk ZnO single crystal grown by flux Bridgman method. Chin. Phys. Lett. **23**(12), 3356 (2006)
26. S.N. Kasarova et al., Analysis of the dispersion of optical plastic materials. Opt. Mater. **29**, 1481 (2007)
27. A.M.S. Galante, L.L. Campos, Characterization of polycarbonate dosimeter for gamma-radiation dosimetry, in *Proceedings of Third European IRPA Congress*, Helsinki, Finland (2010), pp. 14–16
28. M. Aden, Optical properties of polycarbonate. Fraunhofer Institute for Laser Technology ILT. www.ilt.fraunhofer.de
29. A.L. Patterson, The Scherrer formula for X-ray particle size determination. Phys. Rev. **56**, 978 (1939)